EDGE ARTICLE

Check for updates

Stable and reusable Ni-based nanoparticles for general and selective hydrogenation of nitriles to amines†

Zhuang Ma,[a] Vishwas G. Chandrashekhar, [iD][a] Bei Zhou,[a] Asma M. Alenad,[b] Nils Rockstroh, [iD][a] Stephan Bartling, [iD][a] Matthias Beller [iD] *[a] and Rajenahally V. Jagadeesh [iD] *[a]

Silica supported ultrasmall Ni-nanoparticles allow for general and selective hydrogenation of all kinds of nitriles to primary amines under mild conditions. By calcination of a template material generated from Ni(II)nitrate and colloidal silica under air and subsequent reduction in the presence of molecular hydrogen the optimal catalyst is prepared. The prepared supported nanoparticles are stable, can be conveniently used and easily recycled. The applicability of the optimal catalyst material is shown by hydrogenation of >110 diverse aliphatic and aromatic nitriles including functionalized and industrially relevant substrates. Challenging heterocyclic nitriles, specifically cyanopyridines, provided the corresponding primary amines in good to excellent yields. The resulting amines serve as important precursors and intermediates for the preparation of numerous life science products and polymers.

Introduction

Catalytic hydrogenations are a perfect toolbox of chemical reactions with respect to sustainability.[1–5] Besides their 100%-atom economy, the potential use of green hydrogen makes such transformations highly attractive for the future.[1–5] Today, hydrogenations are extensively applied in both research laboratories and industry to provide a variety of fine and bulk chemicals which are used in our daily life.[1–5] As an example, the preparation of the majority of aromatic and many aliphatic amines includes at least one catalytic hydrogenation step.[6–10] The resulting amines are privileged compounds in organic chemistry and find wide-spread applications in synthesis, drug discovery, and agrochemicals as well as for material and energy technologies.[11–13] Among the different kinds of amines, primary ones are particularly interesting, which are commonly prepared by reduction of nitroarenes[6–8] and nitriles,[9,10,14] reductive amination,[15–21] amination of alcohols[22–25] or classic nucleophilic substitution reactions.[26,27]

In the chemical industry, hydrogenation of nitriles are frequently applied to prepare primary benzylic and aliphatic amines on a bulk scale.[9,10,14,28–41] Since the first nitrile hydrogenation of benzonitrile using heterogeneous Ni-catalysts

reported already in 1905,[28] a plethora of materials and molecularly defined complexes based on precious and non-precious metals were developed for this transformation.[9,10,14,29–41] Despite the many applications, most of these catalysts cannot be applied with high activity and selectivity for the hydrogenation of functionalized and structurally complex nitriles, specifically heterocyclic nitriles, which are valuable intermediates for agrochemicals and pharmaceuticals. In such cases, different synthetic steps must be performed to achieve the desired transformation. Hence, there is a continuing interest to improve this methodology by developing new generally applicable catalysts. Ideally, such catalytic materials should be based on 3d-metals due to their availability and price advantages as well as lower toxicity.

In the past decade, we reported Fe-, Co-, and Ni-based supported nanoparticles encapsulated in carbon shells for industrially relevant hydrogenations,[8,38,42] reductive aminations,[15,16] and oxidation processes[43] as well as borrowing hydrogen methodologies.[44] In general, we prepared these materials by pyrolysis of metal complexes or metal–organic frameworks (MOFs) as precursors on heterogeneous supports (Fig. 1).[8,15,16,38,42–44] Compared to these more sophisticated precursors, the use of simple and stable metal salts is more economic and practical (Fig. 1). However, creation of active and selective supported nanoparticles for advanced organic synthesis using simple non-noble metal salts without ligands or additives is very difficult.

Here, we report Ni-nanoparticles generated by calcination of nickel(II) nitrate on silica and subsequent reduction with hydrogen (Fig. 1). The optimal, stable, and reusable catalyst

[a] Leibniz-Institut für Katalyse e.V., Albert-Einstein-Str. 29a, Rostock, D-18059, Germany. E-mail: matthias.beller@catalysis.de; jagadeesh.rajenahally@catalysis.de

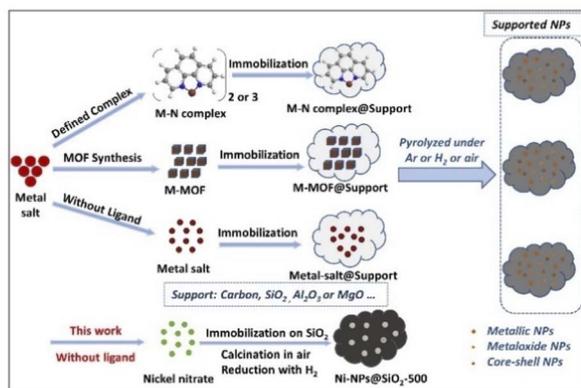*[b] Chemistry Department, College of Science, Jouf University, P.O. Box: 2014, Sakaka, Saudi Arabia*

Fig. 1 Different approaches for the synthesis of supported nanoparticles.

allows for the synthesis of functionalized and structurally complex benzylic, heterocyclic, and aliphatic amines starting from all kinds of nitriles. In particular, we demonstrate the applicability of our catalyst for the hydrogenation of demanding heterocyclic nitriles to the corresponding primary amines.

Results and discussion

Preparation and catalytic evaluation

Initially, we prepared a small library of silica-supported nanoparticles based on 3d-metal nitrates using $Fe(NO_3)_3 \cdot 9H_2O$, $Mn(NO_3)_2 \cdot 4H_2O$, $Co(NO_3)_2 \cdot 6H_2O$, $Ni(NO_3)_2 \cdot 6H_2O$, and $Cu(NO_3)_2 \cdot 3H_2O$. Colloidal silica (LUDOX® HS-40; 40 wt% suspension in H_2O) was used as the precursor for the SiO_2 support. In a typical procedure, we mixed the respective metal nitrate and colloidal silica in water and stirred the mixture for 5 h at 65 °C (Fig. 2).

Then, the water was removed and the remaining solid was dried over night at 110 °C. After calcinations of the metal–SiO_2
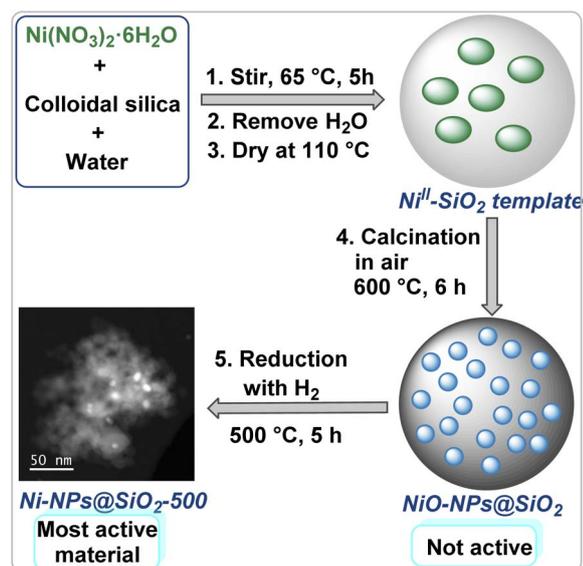

Fig. 2 Preparation of Ni-nanoparticles supported on SiO_2.

templated material under air at 600 °C for 6 h, the respective metal oxides were reduced in presence of molecular hydrogen at 300–700 °C to produce stable silica-supported metallic nanoparticles. The resulting materials are represented as M-NPs@SiO_2-T, where M and T denotes metal and reduction temperature. The details of the synthetic procedure are described in ESI.† Activities and selectivities of all the prepared nanoparticles were evaluated for the hydrogenation of 5-chloropicolinonitrile 1 to (5-chloropyridin-2-yl)methanamine 2 at 80 °C for 24 h (Table 1). This challenging benchmark reaction was chosen due to the importance of halogenated pyridine nitriles for agrochemicals. Notably, traditional hydrogenation catalysts suffer from severe selectivity problems in case of such substrates. Indeed, testing commercially available catalysts such as Ru/C, Pd/C, Pt/C, Rh/C, and RANEY® nickel showed in most cases significant amounts of unwanted dehalogenation reactions and all materials gave only low yield of the desired product 2 (Table 1, entries 1–5). Similarly, our recently reported SiO_2-supported Fe/Fe–O catalyst[14] did not show any activity under these conditions (Table 1, entry 6). Likewise, in the presence of Fe-NPs@SiO_2-500 and Mn-NPs@SiO_2-500 no conversion of 1 was observed (Table 1, entries 7 and 8). Although Co- and Cu-NPs@SiO_2-500 displayed some activity in the model reaction, product yields and selectivities were low (Table 1, entries 9 and 11). However, applying Ni-NPs@SiO_2-500 dramatically improved the reaction and gave 88% yield of (5-chloropyridin-2-yl)methanamine 2 (Table 1, entry 10). Based on these results, several supported Ni-nanoparticles were prepared and tested. As shown in Table 1, catalysts supported on Al_2O_3, TiO_2, and ZnO gave low conversion (<50%), and only traces of (5-chloropyridin-2-yl)methanamine 2 was detected (Table 1, entries 12, 13 and 16).

Using CeO_2 or ZrO_2 supported materials, improved activity was observed, but the selectivity was poor owing to the formation of product 3 and other byproducts (Table 1, entries 14 and 15). Improved conversion for the model reaction was enabled by catalysts immobilized on carbon (Table 1, entry 17). Overall, the silica-supported catalyst outperformed all other materials in terms of selectivity and yield. To evaluate the optimal temperature for the reduction of the nanoparticles, Ni@SiO_2 materials prepared at 400, 500, 600 and 700 °C were compared next (Table 1, entries 18–21). Optimal results were obtained using 500 °C. The material prepared without reduction as well as the non-pyrolyzed one and the precursors exhibited no activity at all (Table 1, entries 22–24). Further, the effect of different solvents, temperature, and other reaction parameters such as hydrogen pressure, amount of catalyst and reaction time were evaluated (Table S1 and Fig. S11, ESI†). Finally, the best result for the benchmark hydrogenation was achieved using 30 mg of Ni-NPs@SiO_2-500 (9 mol% Ni), 35 bar H_2, 5 bar NH_3, at 80 °C in methanol as solvent.

Characterization of Ni-based materials

The prepared Ni-materials were characterized by X-ray powder diffraction (XRD), scanning transmission electron microscopy (STEM), electron energy loss spectroscopy (EELS), and X-ray photoelectron spectroscopy (XPS). XRD patterns of the sample

Table 1 Hydrogenation of 5-chloropicolinonitrile to (5-chloropyridin-2-yl)methanamine: activity of different catalysts[a]
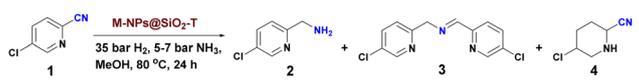
Entry	Catalyst	Conv. of **1** (%)	Yield of **2** (%)	Yield of **3** (%)	Yield of **4** (%)
1	5% Ru/C	99	44	10	11
2	5% Rh/C	99	46	9	9
3	10% Pd/C	99	34	17	16
4	5% Pt/C	99	39	13	13
5	RANEY® Ni	<2	—	<1	—
6[b]	Fe–Fe–O@SiO$_2$	<2	—	<1	—
7	Fe-NPs@SiO$_2$-500	<2	—	<1	—
8	Mn-NPs@SiO$_2$-500	<2	—	<1	—
9	Co-NPs@SiO$_2$-500	50	35	15	—
10	Ni-NPs@SiO$_2$-500	>99	88	11	—
11	Cu-NPs@SiO$_2$-500	41	24	16	—
12	Ni-NPs@Al$_2$O$_3$-500	30	12	17	—
13	Ni-NPs@TiO$_2$-500	32	19	12	—
14	Ni-NPs@CeO$_2$-500	74	47	26	—
15	Ni-NPs@ZrO$_2$-500	65	39	25	—
16	Ni-NPs@ZnO-500	41	22	19	—
17	Ni-NPs@carbon-500	77	61	16	—
18	Ni-NPs@SiO$_2$-300	87	61	26	—
19	Ni-NPs@SiO$_2$-400	91	73	18	—
20	Ni-NPs@SiO$_2$-600	95	80	15	—
21	Ni-NPs@SiO$_2$-700	89	71	18	—
22	NiO@SiO$_2$ calcined under air without reduction	<2	—	<1	—
23[c]	Ni(NO$_3$)$_2$ + SiO$_2$	<2	—	<1	—
24[d]	Ni(NO$_3$)$_2$·6H$_2$O	<2	—	<1	—

[a] Reaction conditions: 0.5 mmol 5-chloropicolinonitrile, 30 mg catalyst (9.0–10 mol% metal), 35 bar H$_2$, 5 bar NH$_3$, 2 mL MeOH, 80 °C, 24 h. [b] Fe-catalyst.[14] [c] Same as 'a' with 9 mol% Ni(NO$_3$)$_2$·6H$_2$O and 15 mg silica. [d] Same as 'a' with 9 mol% Ni(NO$_3$)$_2$·6H$_2$O. Conversion and yield were determined by GC using *n*-hexadecane standard.

calcined at 600 °C (NiO@SiO$_2$ calcined under air) showed the presence of only NiO particles (Fig. S1†).

The patterns for the subsequently reduced materials (Ni-NPs@SiO$_2$-300 Ni-NPs@SiO$_2$-400) displayed the presence of both metallic and oxidic Ni particles, while the ones reduced at 500–700 contained mainly metallic Ni-particles (Fig. S2–S6†). Scanning transmission electron microscopy (STEM) analysis of the materials confirmed the structural changes with increasing temperature (Fig. 3). In all materials, small particles down to 1 nm (Ni-NPs@SiO$_2$-400, Ni-NPs@SiO$_2$-700) or 0.5 nm (Ni-NPs@SiO$_2$-500, Ni-NPs@SiO$_2$-500R (after one run), and Ni-NPs@SiO$_2$-600) are observed. In the case of Ni-NPs@SiO$_2$-600, even single metal atoms were found (Fig. 3E). The larger particles in Ni-NPs@SiO$_2$-400 form irregularly shaped agglomerates up to 250 nm (Fig. 3B). The shape of these agglomerates already changed in Ni-NPs@SiO$_2$-500, where also some spherical Ni containing particles are present (Fig. 3D). Further increase in the reduction temperature led to the formation of exclusively spherical nanoparticles in Ni-NPs@SiO$_2$-700 with sizes of up to 50 nm (Fig. 3H). In addition, some of the Ni containing particles exhibit an oxidic shell around a metallic core (see Fig. 3C top, and S8†). This is most pronounced in sample Ni-NPs@SiO$_2$-500. The combination of all these properties seem to give the most preferable catalytic performance in Ni-NPs@SiO$_2$-500. To proof

the stability (*i.e.*, shape and order of Ni with respect to the support) of the catalytic material, Ni-NPs@SiO$_2$-500 was investigated after one run (Fig. 3I and J). As can be seen, a considerable reorganization of the metal nanoparticles took place under catalytic conditions. The bigger Ni containing entities seem less compact here and additionally, smaller Ni containing particles are formed with considerable amounts of Ni located at the interfaces of the support particles (see Fig. S9†). This is also reflected by the higher surface concentration of Ni observed by XPS (see below). With respect to the oxidation state of Ni, EELS and the contrast of the images suggest an increasing share of metallic nickel with increasing temperature. The difference to the observations from XPS below can be explained by the method itself as XPS probes almost exclusively the surface of the catalysts.

Next, XPS was used to further analyze the catalyst surface. In Table 2 the surface composition of three fresh (pyrolysis temperature 300 °C, 500 °C and 700 °C) and one recycled catalyst are shown in detail. Beside Si and O atoms as main components (as SiO$_2$) small amounts of Ni and C as well as Na and F can be detected. The latter two are probably originated in the catalyst preparation procedure and/or sample handling. However, the Ni concentration is quite similar in the fresh catalysts (between 0.5 to 0.7 at%), whereas the recycled catalyst
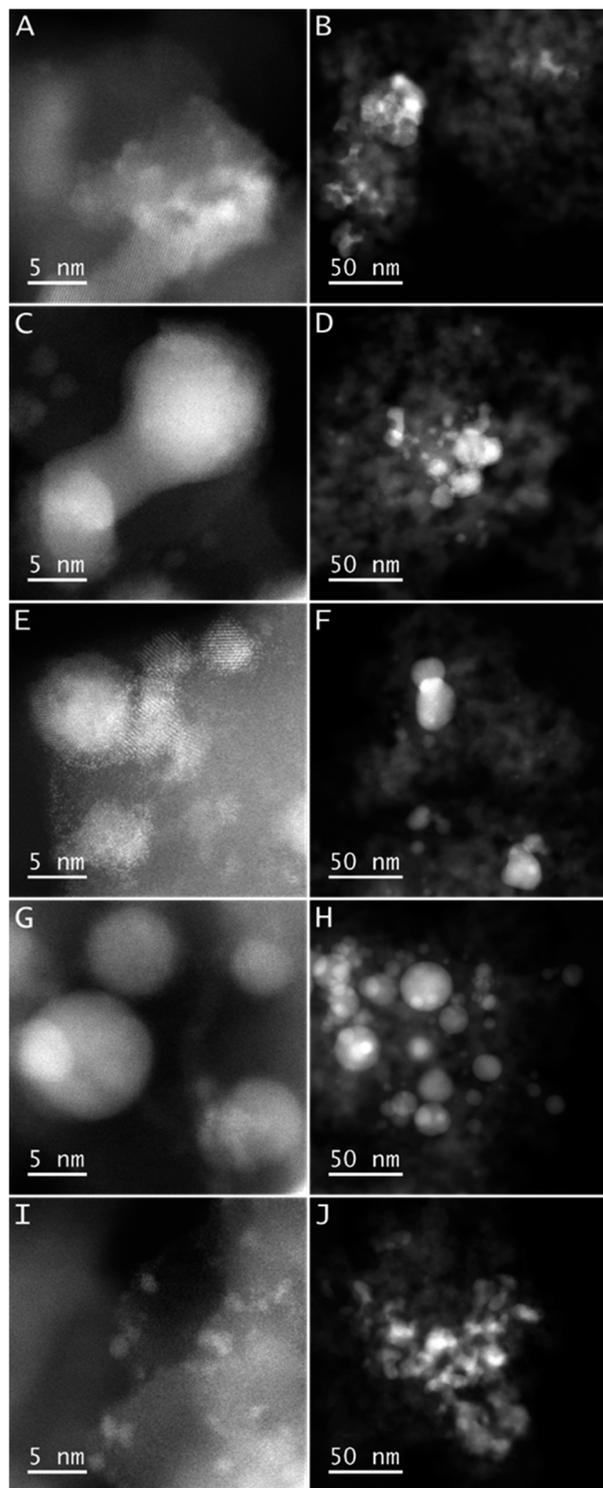
Fig. 3 STEM-HAADF (high-angle annular dark-field) images of Ni-NPs@SiO$_2$-400 (A and B), Ni-NPs@SiO$_2$-500 (C and D), Ni-NPs@SiO$_2$-600 (E and F), Ni-NPs@SiO$_2$-700 (G and H), and Ni-NPs@SiO$_2$-500R (after one run) (I and J).

shows a higher Ni concentration of 1.8 at% which might be correlated to the reorganization of the Ni particles observed by TEM. The Ni 2p spectra of these four catalysts are shown in Fig. 4 and reveal a main doublet around ∼855 eV and ∼873 eV

Table 2 Surface composition of the catalysts obtained by XPS. All values are given in at%

Catalyst	Si	O	Ni	C	Na	F
Ni-NPs@SiO$_2$-300	35.0	61.5	0.7	0.9	1.1	0.8
Ni-NPs@SiO$_2$-500	33.9	61.3	0.5	2.7	1.4	—
Ni-NPs@SiO$_2$-700	35.9	61.1	0.5	1.43	1.1	—
Ni-NPs@SiO$_2$-500R	29.3	51.9	1.8	8.4	—	8

which is characteristic for Ni 2p$_{3/2}$ and Ni 2p$_{5/2}$ in the oxidation state +2 together with strong satellite features at slightly higher binding energies.[45,46] At the lower binding energy side around 852.5 eV a signal corresponding to metallic Ni can be observed.[46] Whereas Ni-NPs@SiO$_2$-300 and Ni-NPs@SiO$_2$-700 (Fig. 4A and B) show a mainly oxidic Ni surface (relative metal concentration 3.3 at% and 9.9 at%, respectively), the highest relative metal concentration of about 13% can be observed for Ni-NPs@SiO$_2$-500 (see Fig. 4C). For the recycled catalyst Ni-NPs@SiO$_2$-500R almost no metallic Ni is observed which goes hand in hand with the structural changes seen by TEM. It is worth mentioning that the Ni 2p binding energies for Ni-NPs@SiO$_2$-500 and Ni-NPs@SiO$_2$-500R are shifted to significantly higher values by about 2 eV. This indicates a much stronger interaction of nickel with the support which can also result in the formation of nickel silicate at the surface with similar binding energies as found here.[47,48] STEM and XRD results show no evidence for the formation of nickel silicate. However, the observed binding energy shift might be a consequence of the pyrolysis temperature of 500 °C, which also leads to the highest activity in the catalytic experiments. Concluding from the analysis by STEM and XPS, a significant amount of metallic nickel as well as a sufficiently high interaction between the support and Ni seem to be an important prerequisite for the synthesis of a well-performing catalyst. Moreover, the reorganization of the material after one run implies that the presence of interfaces between SiO$_2$ crystallites is crucial for the formation and deposition of small Ni containing entities. This formation may be linked both to the Ni containing particle's size, shape, and composition, as well as to the size of the SiO$_2$ crystallites of the freshly prepared materials.
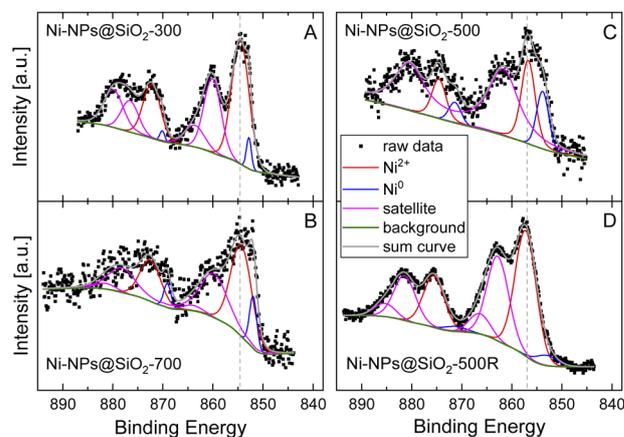

Fig. 4 XPS spectra of the Ni 2p region of Ni@SiO$_2$-300 (A), Ni@SiO$_2$-700 (B), Ni@SiO$_2$-500 (C), and Ni@SiO$_2$-500R (D).
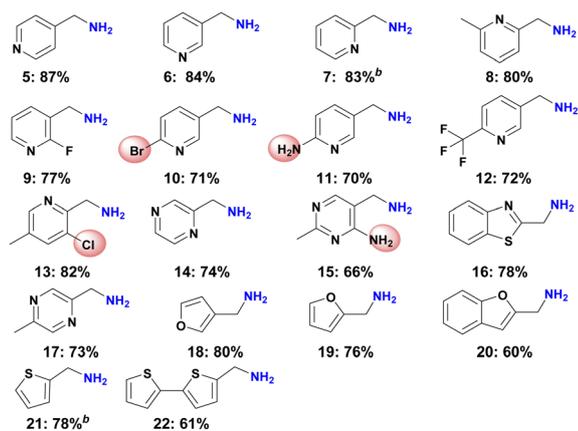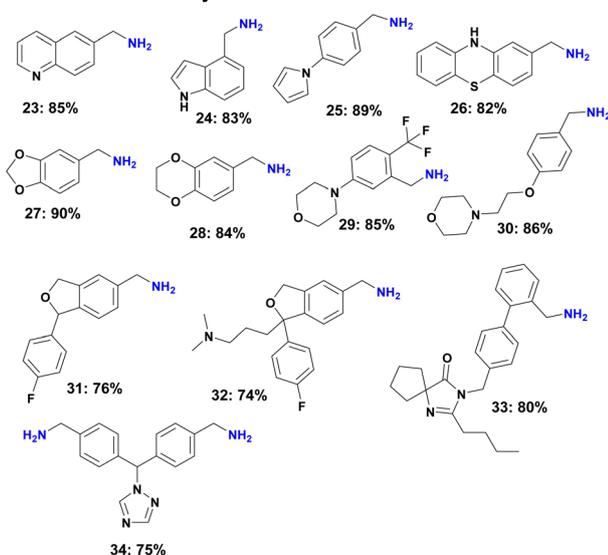
Synthetic applications

With a most active catalyst (Ni@SiO$_2$-500) for the selective hydrogenation of 5-chloropicolinonitrile in hand, we explored its general applicability for the synthesis of primary amines from all kinds of aromatic and aliphatic nitriles. First, we performed the hydrogenation of heteroarene nitriles.

Hydrogenation of heteroarene nitriles and nitriles with heterocyclic substituents. The resulting amines are an important class of compounds, which are used as intermediates in the pharmaceutical and agrochemical industries. As a result, pyridyl-based nitriles containing different additional substituents including F-, Cl-, Br-, CF$_3$-, and NH$_2$- were smoothly reduced (Scheme 1, products **5–13**). Similarly, other cyano-substituted heterocycles including pyrimidines, thiazoles, furans, and thiophenes gave the corresponding products in good to very good yield without further optimizations (Scheme 1, products **14–22**).

In addition, other nitriles with heterocyclic substituents such as quinoline, indole, pyrrole, thiazine, benzodioxol, benzodioxane, morpholine, tetrahydrofuran, as well as imidazole and triazole were selectively hydrogenated and produced the corresponding heterocyclic amines in up to 90% (Scheme 1, products **23–34**).

Hydrogenation of aromatic nitriles. As shown in Scheme 2, common benzonitriles including ones bearing additional aromatic or alkyl groups gave the desired benzylic amines in up to 94% yield (Scheme 2, products **35–39**).

To demonstrate the chemoselectivity of this novel Ni-based catalyst system more clearly, the hydrogenation of nitriles
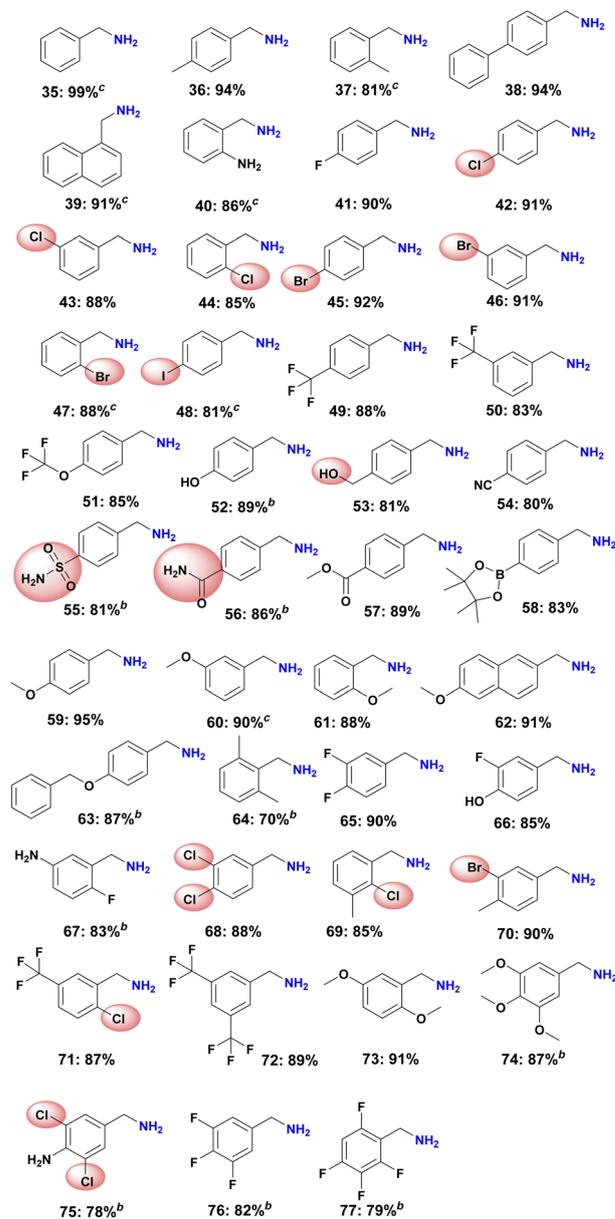
Scheme 1 Ni-NPs@SiO$_2$-500 catalyzed hydrogenation of heterocyclic nitriles.[a] Reaction conditions: [a] 0.5 mmol nitrile, 30 mg Ni-NPs@SiO$_2$-500 (9 mol% Ni), 35 bar H$_2$, 5 bar NH$_3$, 2 mL MeOH, 80 °C, 24 h. Isolated as free amines and converted to hydrochloride salts for measuring NMR. [b] GC yields using n-hexadecane standard.
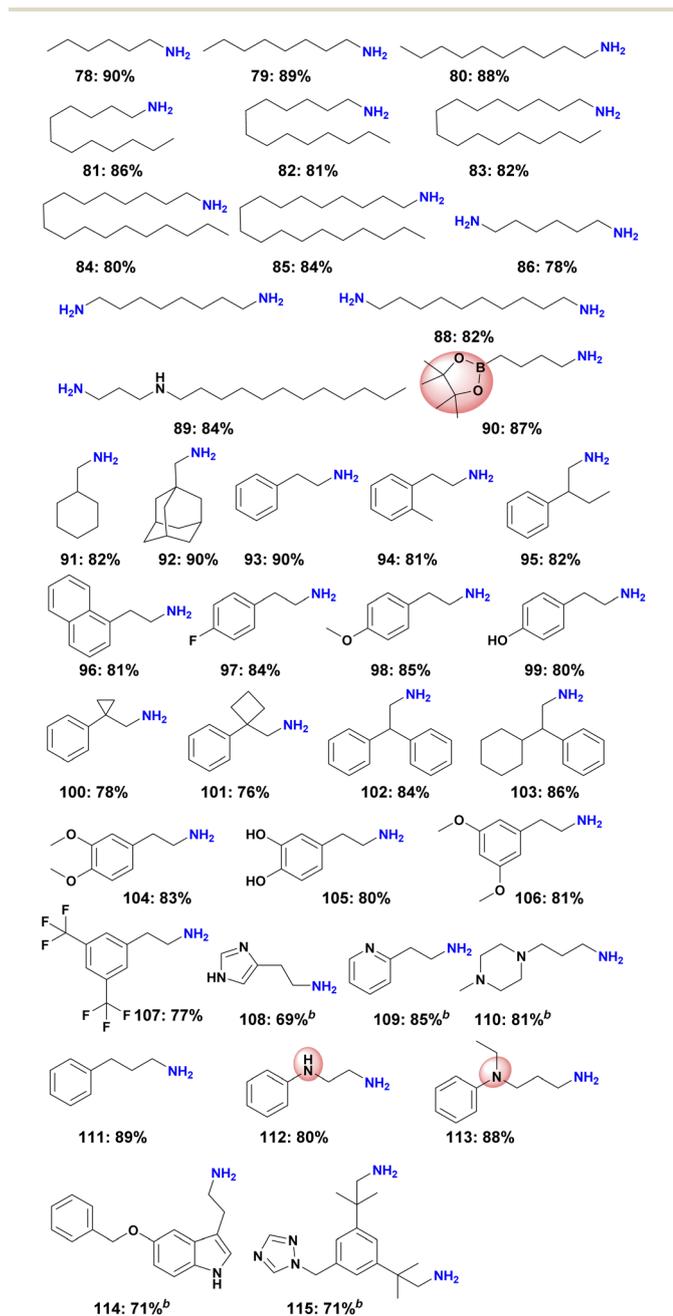
Scheme 2 Ni-NPs@SiO$_2$-500 catalyzed hydrogenation of aromatic nitriles.[a] Reaction conditions: [a] 0.5 mmol nitrile, 15 mg Ni-NPs@SiO$_2$-500 (4.5 mol% Ni), 35 bar H$_2$, 5 bar NH$_3$, 2 mL MeOH, 60 °C, 18 h, isolated yields. Isolated as free amines and converted to hydrochloride salts for measuring NMR. [b] Same as 'a' at 80 °C. [c] GC yields using n-hexadecane standard.

with sensitive functional groups was investigated in detail. In consequence several halogenated benzylic amines as well as amino- and trifluoromethyl-substituted ones (Scheme 2, products **40–50**) were prepared, which are known to be versatile intermediates in organic synthesis. No dehalogenation products were detected for fluoro-, chloro-, and bromide-substituted substrates, whereas a small amount of dehalogenation product was observed for the iodine-containing substrates. In addition, aromatic nitriles with trifluoromethoxy, hydroxyl, amide, ester

as well as boronic ester and ether groups were also selectively hydrogenated and gave smoothly the corresponding primary amines (Scheme 2, products **51–63**). Finally, a range of multi-substituted benzylic amines were prepared using Ni-NPs@SiO$_2$-500 in up to 91% yield from the corresponding nitriles (Scheme 2, products **64–77**).

Hydrogenation of aliphatic nitriles. Compared to aromatic nitriles, the hydrogenation of araliphatic and aliphatic nitriles, especially in the presence of non-noble metal catalysts, typically needs high temperature and pressure. However, performing the hydrogenation of a range of aliphatic nitriles in the presence of Ni-NPs@SiO$_2$-500 the corresponding primary amines are obtained in good to excellent yield already at 80 °C (Scheme 3). Apart from high activity at low temperature, our catalyst material also exhibited for this type of substrates high selectivity towards the desired primary amines even for industrially important di-nitriles (Scheme 3, products **86–88**). More specifically, hexamethylenedi-amine, a key feedstock to produce nylon 66, is prepared in 78% yield by direct hydrogenation of adiponitrile. Other substituted nitriles were also smoothly hydrogenated and offered the corresponding fluoro-, methoxy-, hydroxyl-, cyclopropyl-, cyclobutyl-, as well as trifluoromethyl- and amino-substituted primary amines in up to 89% yield (Scheme 3, products **97–115**).
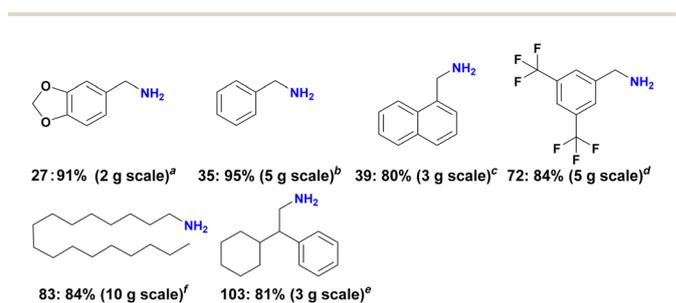
Demonstrating practicability

Further to showcase the synthetic utility and practicality of our Ni catalyst, we performed six scale-up experiments with selected nitriles up to 10 g scale. As shown in Scheme 4, all hydrogenations proceeded smoothly, and in all cases yields similar to mg-scale reactions were obtained.

Finally, to demonstrate the stability and reusability of the optimal catalyst material, recycling experiments were conducted for the model reaction under two different conditions (20 h, complete conversion and 7 h, about 50% conversion). Gratifyingly, Ni-NPs@SiO$_2$-500 exhibited good stability and could be recycled and reused for eight times with only slight deactivation (Fig. 5).

The general reaction pathway for catalytic hydrogenations of nitriles to amines is shown in Fig. S11a.†

Scheme 3 Ni-NPs@SiO$_2$-500 catalyzed hydrogenation of aliphatic and fatty nitriles.[a] Reaction conditions: [a] 0.5 mmol nitrile, 20 mg Ni-NPs@SiO$_2$-500 (6.0 mol% Ni), 35 bar H$_2$, 5 bar NH$_3$, 2 mL MeOH, 80 °C, 24 h, isolated yield. Isolated as free amines and converted to hydro-chloride salts for measuring NMR. [b] Same as 'a' with 30 mg Ni-NPs@SiO$_2$-500 (9.0 mol% Ni).

Scheme 4 Ni-NPs@SiO$_2$-500 catalyst for upscale reaction. Reaction conditions: [a] 780 mg Ni-NPs@SiO$_2$-500 (9.0 mol% Ni), 35 bar H$_2$, 5 bar NH$_3$, 30 mL MeOH, 80 °C, 24 h; [b] 1.4 g Ni-NPs@SiO$_2$-500 (4.5 mol% Ni), 35 bar H$_2$, 5 bar NH$_3$, 30 mL MeOH, 60 °C, 24 h; [c] same as 'b' with 500 mg Ni-NPs@SiO$_2$-500 (4.5 mol% Ni); [d] same as 'b' with 615 mg Ni-NPs@SiO$_2$-500 (4.5 mol% Ni); [e] same as 'a' with 580 mg Ni-NPs@SiO$_2$-500 (6.0 mol% Ni); [f] same as 'a' with 1.5 g Ni-NPs@SiO$_2$-500 (6.0 mol% Ni). Isolated yields.
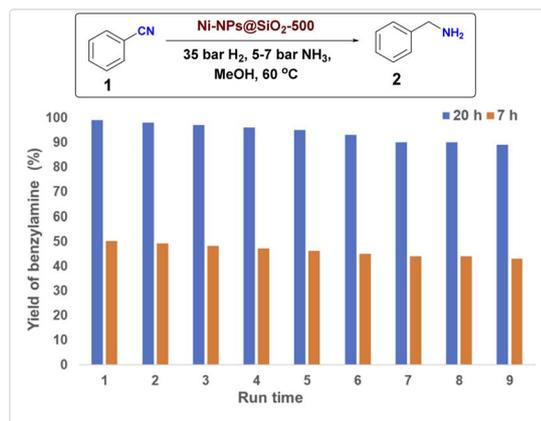
Fig. 5 Stability and recycling of Ni-NPs@SiO$_2$-500 catalyst for the hydrogenation of benzonitrile to benzylamine. Reaction conditions: 10 mmol benzonitrile, 320 mg Ni-NPs@SiO$_2$-500 (4.8 mol% Ni), 35 bar H$_2$, 5 bar NH$_3$, 40 mL MeOH, 60 °C, 20 h and 7 h, GC yields using *n*-hexadecane standard.

Conclusions

In conclusion, we report the use of ultrasmall nickel nanoparticles supported on silica as a most general heterogeneous catalyst for the selective hydrogenation of all kinds of nitriles to primary amines under mild conditions. This catalyst can be easily handled and allows for selective hydrogenation of demanding substrates, thereby offering an efficient straightforward route towards heterocyclic primary amines, which represent valuable building blocks, especially for the synthesis of agrochemicals and other bio-active compounds. The optimal catalyst material is conveniently prepared by calcination of an inexpensive template material generated from Ni-nitrate and colloidal silica under air. After subsequent reduction in presence of molecular hydrogen the resulting supported ultrasmall Ni nanoparticles are highly stable and recyclable.

Data availability

All data associated with this article have been included in the main text and ESI.†

Author contributions

RVJ and MB supervised the project. ZM, RVJ and MB planned and developed the project. ZM prepared catalytic materials and performed catalytic experiments. VGC and BZ co-performed catalytic experiments and reproduced the results. AMA involved in the development of this project. NR and SB performed TEM and XPS analysis. ZM, VGC, BZ, MB and RVJ wrote the paper with the contribution of NR and SB.

Conflicts of interest

There are no conflicts to declare.

Notes and references

1 A. M. Oliveira, R. R. Beswick and Y. Yan, A green hydrogen economy for a renewable energy society, *Curr. Opin. Chem. Eng.*, 2021, **33**, 100701.

2 S. Nishimura, *Handbook of Heterogeneous Catalytic Hydrogenation for Organic Synthesis*, Wiley, New York, 2001.

3 J. G. de Vries and C. J. Elsevier, *Handbook of Homogeneous Hydrogenation*, Weinheim Wiley-VCH, 2007.

4 A. M. Smith and R. Whyman, Review of methods for the catalytic hydrogenation of carboxamides, *Chem. Rev.*, 2014, **114**, 5477–5510.

5 L. Zhang, M. Zhou, A.-Q. Wang and T. Zhang, Selective hydrogenation over supported metal catalysts: from nanoparticles to single atoms, *Chem. Rev.*, 2019, **120**, 683–733.

6 D. Formenti, F. Ferretti, F. K. Scharnagl and M. Beller, Reduction of nitro compounds using 3d-non-noble metal catalysts, *Chem. Rev.*, 2018, **119**, 2611–2680.

7 A. Corma and P. Serna, Chemoselective hydrogenation of nitro compounds with supported gold catalysts, *Science*, 2006, **313**, 332–334.

8 R.-V. Jagadeesh, A.-E. Surkus, H. Junge, M.-M. Pohl, J. Radnik, J. Rabeah, H. Huan, V. Schünemann, A. Brückner and M. Beller, Nanoscale Fe$_2$O$_3$-based catalysts for selective hydrogenation of nitroarenes to anilines, *Science*, 2013, **342**, 1073–1076.

9 B.-B. Dattatraya and M.-B. Bhalchandra, Recent advances in transition metal-catalyzed hydrogenation of nitriles, *Adv. Synth. Catal.*, 2015, **357**, 883–900.

10 Q. Lua, J. Liu and L. Ma, Recent advances in selective catalytic hydrogenation of nitriles to primary amines, *J. Catal.*, 2021, **404**, 475–492.

11 S. A. Lawrence, *Amines: synthesis, Properties and Applications*, Cambridge Univ. Press, 2004.

12 A. Ricci, *Amino Group Chemistry: From Synthesis to the Life Sciences*, Wiley-VCH, 2008.

13 M. H. Qureshi, *Top 200 Pharmaceuticals by Retails Sales in 2020*, University of Arizona, 2020, **https://njardarson.lab.arizona.edu/sites/njardarson.lab.ariona.edu/fles/Top%20200%20Pharmaceutcals%20By%20Retail%20Sales%2020 20V3.pdf**.

14 V. G. Chandrashekhar, T. Senthamarai, R. G. Kadam, O. Malina, J. Kašlík, R. Zbořil, M.-B. Gawande, R.-V. Jagadeesh and M. Beller, Silica-supported Fe/Fe-O

nanoparticles for the catalytic hydrogenation of nitriles to amines in the presence of aluminium additives, *Nat. Catal.*, 2022, **5**, 20–29.

15 R.-V. Jagadeesh, K. Murugesan, A.-S. Alshammari, H. Neumann, M.-M. Pohl, J. Radnik and M. Beller, MOF-derived cobalt nanoparticles catalyze a general synthesis of amines, *Science*, 2017, **358**, 326–332.

16 K. Murugesan, M. Beller and R.-V. Jagadeesh, Reusable nickel nanoparticles-catalyzed reductive amination for selective synthesis of primary amines, *Angew. Chem., Int. Ed.*, 2019, **58**, 5064–5068.

17 K. Murugesan, T. Senthamarai, V.-G. Chandrashekhar, K. Natte, P. C. Kamer, M. Beller and R.-V. Jagadeesh, *Chem. Soc. Rev.*, 2020, **49**, 6273–6328.

18 T. Irrgang and R. Kempe, Transition-metal-catalyzed reductive amination employing hydrogen, *Chem. Rev.*, 2020, **120**, 9583–9674.

19 G. Hahn, P. Kunnas, N. de Jonge and R. Kempe, General synthesis of primary amines *via* reductive amination employing a reusable nickel catalyst, *Nat. Catal.*, 2019, **2**, 71–77.

20 O.-I. Afanasyev, E. Kuchuk, D.-L. Usanov and D. Chusov, Reductive amination in the synthesis of pharmaceuticals, *Chem. Rev.*, 2019, **119**, 11857–11911.

21 H.-F. Qi, J. Yang, F. Liu, L. Zhang, J.-Y. Yang, X. Liu, L. Li, Y. Su, Y.-F. Liu, R. Hao, A.-Q. Wang and T. Zhang, Highly selective and robust single-atom catalyst Ru/NC for reductive amination of aldehydes/ketones, *Nat. Commun.*, 2021, **12**, 1–11.

22 T. Irrgang and R. Kempe, 3d-metal catalyzed N- and C-alkylation reactions *via* borrowing hydrogen or hydrogen autotransfer, *Chem. Rev.*, 2019, **119**, 2524–2549.

23 A. Corma, J. Navas and M. Sabater, Advances in one-pot synthesis through borroing hydrogen catalysis, *Chem. Rev.*, 2018, **118**, 1410–1459.

24 T. Yan, B.-L. Feringa and K. Barta, Iron catalysed direct alkylation of amines with alcohols, *Nat. Commun.*, 2014, **5**, 1–7.

25 F. Shi and X.-J. Cui, *Catalytic Amination for N-Alkyl Amine Synthesis*, Academic Press, 2018.

26 P.-R. Castillo and S.-L. Buchwald, Applications of palladium catalyzed C–N cross-coupling reactions, *Chem. Rev.*, 2016, **116**, 12564–12649.

27 J.-F. Hartwig, Evolution of a fourth generation catalyst for the amination and thioetherification of aryl halides, *Acc. Chem. Res.*, 2008, **41**, 1534–1544.

28 P. Sabatier and J.-B. Senderens, Application aux nitriles de la methode d'hydrogenation directe par catalyse: synthese d'amines primaires, secondaires et tertiaires, *C. R. Hebd. Seances Acad. Sci.*, 1905, **140**, 482–484.

29 M. Freifelder, A low pressure process for the reduction of nitriles. Use of rhodium catalyst, *J. Am. Chem. Soc.*, 1960, **82**, 2386–2389.

30 L.-K. Freidlin and T.-A. Sladkova, Catalytic reduction of dinitriles, *Russ. Chem. Rev.*, 1964, **33**, 319–330.

31 C. Barnett, Hydrogenation of aliphatic nitriles over transition metal borides, *Ind. Eng. Chem. Prod. Res. Dev.*, 1969, **8**, 145–149.

32 C. de Bellefon and P. Fouilloux, Homogeneous and heterogeneous hydrogenation of nitriles in a liquid phase: chemical, mechanistic, and catalytic aspects, *Catal. Rev.*, 1994, **36**, 459–506.

33 Y.-M. López-De Jesús, C.-E. Johnson, J.-R. Monnier and C.-T. Williams, Selective hydrogenation of benzonitrile by alumina-supported Ir–Pd catalysts, *Top. Catal.*, 2010, **53**, 1132–1137.

34 K. Lévay and L. Hegedűs, Recent achievements in the hydrogenation of nitriles catalyzed by transitional metals, *Curr. Org. Chem.*, 2019, **23**, 1881–1900.

35 M. Yoshimura, A. Komatsu, M. Niimura, Y. Takagi, T. Takahashi, S. Ueda, T. Ichikawa, Y. Kobayashi, H. Okami and T. Hattori, Selective synthesis of primary amines from nitriles under hydrogenation conditions, *Adv. Synth. Catal.*, 2018, **360**, 1726–1732.

36 Y. Liu, S. He, Z. Quan, H. Cai, Y. Zhao and B. Wang, Mild palladium catalysed highly efficient hydrogenation of $C\equiv N$, $C–NO_2$, and $C=O$ bonds using H_2 of 1 atm in H_2O, *Green Chem.*, 2019, **21**, 830–838.

37 H. Wang, Q. Luo, W. Liu, Y. Lin, Q. Guan, X. Zheng, H. Pan, J. Zhu, Z. Sun and S. Wie, Quasi Pd_1Ni single-atom surface alloy catalyst enables hydrogenation of nitriles to secondary amines, *Nat. Commun.*, 2019, **10**, 4998.

38 P. Ryabchuk, G. Agostini, M.-M. Pohl, H. Lund, A. Agapova, H. Junge, K. Junge and M. Beller, Intermetallic nickel silicide nanocatalyst: A non-noble metal-based general hydrogenation catalyst, *Sci. Adv.*, 2018, **4**, eaat0761.

39 K. Murugesan, T. Senthamarai, M. Sohail, A.-S. Alshammari, M.-M. Pohl, M. Beller and R.-V. Jagadeesh, Cobalt-based nanoparticles prepared from MOF–carbon templates as efficient hydrogenation catalysts, *Chem. Sci.*, 2018, **9**, 8553–8560.

40 T. Mitsudome, M. Sheng, A. Nakata, T. Mizugaki and K. Jitsukawa, A cobalt phosphide catalyst for the hydrogenation of nitriles, *Chem. Sci.*, 2020, **11**, 6682–6689.

41 S. Enthaler, K. Junge and M. Beller, Sustainable metal catalysis with iron: from rust to a rising star, *Angew. Chem., Int. Ed.*, 2008, **47**, 3317–3321.

42 K. Murugesan, V.-G. Chandrashekhar, C. Kreyenschulte, M. Beller and R.-V. Jagadeesh, A general catalyst based on cobalt core-shell nanoparticles for the hydrogenation of N-heteroarenes including pyridines, *Angew. Chem., Int. Ed.*, 2020, **59**, 17408–17412.

43 T. Senthamarai, V.-G. Chandrashekhar, N. Rockstroh, J. Rabeah, S. Bartling, R.-V. Jagadeesh and M. Beller, A "universal" catalyst for aerobic oxidations to synthesize (hetero) aromatic aldehydes, ketones, esters, acids, nitriles, and amides, *Chem*, 2022, **8**, 508–531.

44 Z. Ma, B. Zhou, X.-M. Li, R.-G. Kadam, M. B Gawande, M. Petr, R. Zbořil, M. Beller and R.-V. Jagadeesh, Reusable Co-nanoparticles for general and selective N-alkylation of amines and ammonia with alcohols, *Chem. Sci.*, 2022, **13**, 111–117.

45 A.-P. Grosvenor, M.-C. Biesinger, R. S.-C. Smart and N.-S. McIntyre, New interpretations of XPS spectra of nickel metal and oxides, *Surf. Sci.*, 2006, **600**, 1771–1779.

46 M.-C. Biesinger, B.-P. Payne, L.-W. Lau, A. Gerson and R. S.-C. Smart, X-ray photoelectron spectroscopic chemical state quantification of mixed nickel metal, oxide and hydroxide systems, *Surf. Interface Anal.*, 2009, **41**, 324–332.

47 C. Wagner, L. Gale and R. Raymond, Two-dimensional chemical state plots: a standardized data set for use in identifying chemical states by x-ray photoelectron spectroscopy, *Anal. Chem.*, 1979, **51**, 466–482.

48 X. Lu, M.-A. Baker, D.-H. Anjum, G. Basina, S.-J. Hinder, W. Papawassiliou, A.-J. Pell, M. Karagianni, G. Papavassiliou and D. Shetty, Ni_2P Nanoparticles Embedded in Mesoporous SiO_2 for Catalytic Hydrogenation of SO_2 to Elemental S, *ACS Appl. Nano Mater.*, 2021, **4**, 5665–5676.